Available online at www.sciencedirect.com

ScienceDirect

IFAC PapersOnline CONFERENCE PAPER ARCHIVE

IFAC PapersOnLine 52-5 (2019) 411–416

Modelling and efficiency formulation of a planetary traction drive CVT

Michele Tomaselli * **Paolo Lino** * **Giuseppe Carbone** **

* *Dipartimento di Ingegneria Elettrica e dell'Informazione, Politecnico di Bari, Via Re David 200, 70125 Bari, Italy (e-mail: michele.tomaselli@poliba.it, paolo.lino@poliba.it)*

** *Dipartimento di Ingegneria Meccanica e Management, Politecnico di Bari, Viale Japigia 182 - 70126 Bari (e-mail: giuseppe.carbone@poliba.it)*

Abstract: In this paper, we present the model in steady state conditions of a planetary traction drive continuously variable transmission (CVT). The model provides the efficiency formulation of the CVT as a function of the geometry, and the operative point considering slip and spin losses in the points of contact. The physical behaviour has been studied using the results from the EHL theory. The simulation results of this model show good efficiency performances and a large reduction ratio range.

Keywords: Continuously variable transmission; Modelling; Physical models; Efficiency; Transmission; Static model

1. INTRODUCTION

The dedication to green technology and the environmental care from society and governments have increased exponentially in the recent years. Car manufacturers must face with rules and technology constraints that became more and more strictly. For these reasons, researchers and engineers have focused their works on the improvements, in terms of emissions and fuel reduction, of the internal combustion engines. One of the most promising solution to improve these performances is the adoption of a Continuously Variable Transmission (CVT). These transmissions can vary their speed ratios in a continuous and smooth way. Such characteristic is useful for reducing the fuel consumption in traditional internal combustion engines. Carbone et al. (2001) analysed the impact of the adoption of different CVT architecture in a mid-class of passenger car. Furthermore, a variable transmission can be used in hybrid powertrain to manage their complex architecture. Bottiglione et al. (2014) showed that in a pure electric vehicle, the adoption of a CVT transmission can improve efficiency performances.

In this work, we propose a steady state model of a novel CVT traction drive also known as *NuVinci* in the commercial application. In these transmissions, a so called *traction oil* is used to transmit power through the CVT. Due to its rheological properties, the viscosity of the traction oil increases under high contact pressure. In this way, there is no need of belt, chain or teeth meshing. Without these mechanical constraints, the transmission ratio can be changed by varying the angle between the axes of rotation Carbone et al. (2007). Our model provides the efficiency curves of the transmission in terms of speed and torque efficiency. The speed efficiency is affected by slip between the contact bodies, while the torque efficiency is affected by spin and bearing losses. The steady state model can be generalized for dynamic condition by including the inertia of rotating bodies to evaluate the variation of angular speed and transmission ratio (Verbelen et al. (2018)).

2. KINEMATIC ANALYSIS

2.1 Geometrical description

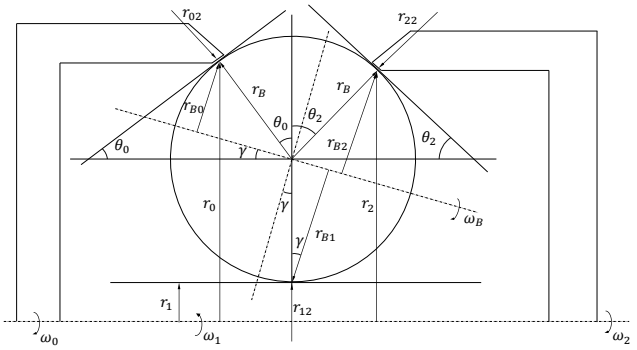

Fig. 1. CVT Geometrical quantities

The scheme in Fig. 1 shows the main geometrical quantities of the transmission. In this figure, θ_0, θ_1 and θ_2 are the angles between the horizontal axis and the tangent at the roller passing through the three points of contact, respectively with input disk, sun shaft and output disk. In the same figure, γ is the angle between the horizontal axis and the rotation axis of the roller (here in after *Tilt Angle*). Moreover r_{02}, r_{12}, r_{22} are the second principal radii of curvature along the tangential direction for the three points of contact. Finally, r_1 is the radius of the sun shaft. This shaft is free to move and is used to keep the rollers in contact with the disks. As shown in Fig. 1, the disks meet each roller in three points.

2405-8963 © 2019, IFAC (International Federation of Automatic Control) Hosting by Elsevier Ltd. All rights reserved.
Peer review under responsibility of International Federation of Automatic Control.
10.1016/j.ifacol.2019.09.066

According to the geometry of the transmission, the following relations hold true:

$$r_{B0} = r_B cos(\theta_1 + \gamma) \quad (1)$$
$$r_{B1} = r_B cos(\gamma) \quad (2)$$
$$r_{B2} = r_B cos(\theta_2 - \gamma) \quad (3)$$

Similarly, r_0 and r_2 can be written as:

$$r_0 = r_1 + r_B + r_B cos(\theta_0) = r_B[1 + k + cos(\theta_0)] \quad (4)$$
$$r_2 = r_1 + r_B + r_B cos(\theta_2) = r_B[1 + k + cos(\theta_2)] \quad (5)$$

where $k = r_1/r_B$ is defined as the *Aspect Ratio*. Here in after, these parameters will be express in a dimensionless form with respect to the roller radius r_B. For example, a generic variable x will be expressed as $x = \tilde{x} r_B$.

2.2 Reduction ratio

For each value of γ, the CVT can be analysed as a two-stage planetary transmission. Fig. 2 shows a schematic view of the transmission. This figure explains the analogy with a planetary gearset in which the planets radii are not constant and the carrier is locked. In ideal conditions, the following relations hold true:

$$\begin{aligned} \omega_0 r_0 &= \omega_B r_{B0} \\ \omega_2 r_2 &= \omega_B r_{B2} \end{aligned} \quad (6)$$

Combining equations (1) - (6), we are able to define the reduction ratio as a function of the tilt angle γ:

$$\tau_{ID} = \frac{\omega_2}{\omega_0} = \frac{r_{B2} r_0}{r_{B0} r_2} = \frac{cos(\theta_2 - \gamma)[1 + k + cos(\theta_0)]}{cos(\theta_0 + \gamma)[1 + k + cos(\theta_2)]} = \\ = \tau_0 \frac{cos(\theta_2 - \gamma)}{cos(\theta_0 + \gamma)} \quad (7)$$

If $\theta_0 = \theta_2 = \theta$, the reduction ratio becomes:

$$\tau = \frac{cos(\theta - \gamma)}{cos(\theta + \gamma)} \quad (8)$$

The evaluation of the reduction ratio range needs the definition of an admissible range for tilt angle. Referring to Fig. 1, the following conditions hold true:

$$\gamma > max\left(-\theta_0, \left[\theta_2 - \frac{\pi}{2}\right]\right)$$
$$\gamma < min\left(\theta_2, \left[\frac{\pi}{2} - \theta_0\right]\right) \quad (9)$$

Fig. 3 shows the ideal reduction ratios at different values of θ. Obviously, constraints shown in (9) derive from pure geometrical considerations. In a practical implementation, this range should consider the tilt angle actuation system and the bearing on the rollers. In our model, this range has been reduced by introducing a safety factor of 0.8.

2.3 Creep and spin losses

As will be shown in the next sections, the transmission of torque is due to the difference of tangential speed in the region of contact between the rotating bodies. For this reason, in real devices a little amount of creep is always present. To evaluate the transmission in presence

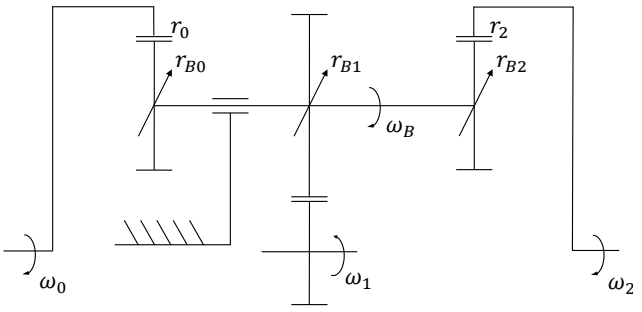

Fig. 2. Schematic view of the CVT

of creep, we define the creep coefficients C_{R0}, C_{R1} and C_{R2} as follows:

$$C_{R0} = \frac{|\omega_0| r_0 - |\omega_B| r_{B0}}{|\omega_0| r_0} \quad (10)$$
$$C_{R1} = \frac{|\omega_B| r_{B1} - |\omega_1| r_1}{|\omega_B| r_{B1}} \quad (11)$$
$$C_{R2} = \frac{|\omega_B| r_{B2} - |\omega_2| r_2}{|\omega_B| r_{B2}} \quad (12)$$

Considering the creep coefficients, we can rephrase the reduction ratio in eq. 7 as:

$$\tau_R = \frac{\omega_2 \omega_B}{\omega_B \omega_0} = \frac{r_0 r_{B2}}{r_{B0} r_2}(1 - C_{R0})(1 - C_{R2}) = \\ = \tau_{ID}(1 - C_{R0})(1 - C_{R2}) \quad (13)$$

Creep can be thought as a loss in transmission of speed through the CVT. In this way, we can define the efficiency of the CVT in terms of speed transmission:

$$\eta_{Speed} = \frac{\tau_R}{\tau_{ID}} = (1 - C_{R0})(1 - C_{R2}) \quad (14)$$

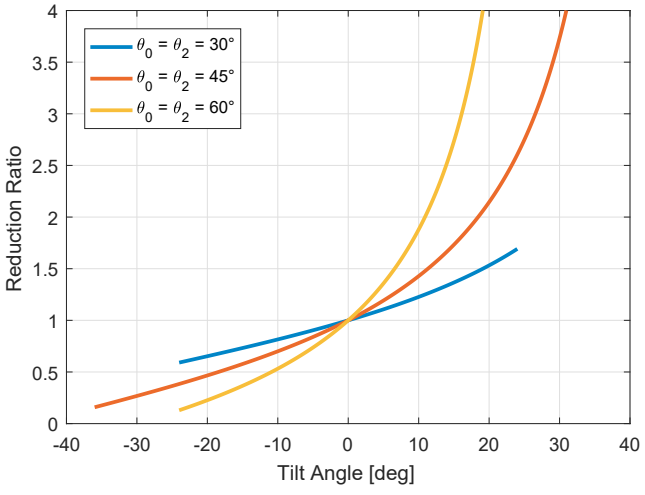

Fig. 3. Reduction ratio at different values of $\theta_0 = \theta_2$

Spin consists of parasitic axis of rotation that acts along normal direction in the point of contact between two rotating bodies. It causes losses in torque transmission and can generate considerable side forces on the rotating bodies Loewenthal (1986). Carbone et al. (2007) have developed a model of the Half-Toroidal CVT that takes

into account this effect. Morover, S. Cretu and P. Glovnea (2003) explained with more details this phenomena and proposed a so colled *Spin-Friendly* design of a spherical-roller transmission quite similar to the one proposed in our works, in which the external disks meet the roller on its lower side. Considering the angular velocity defined in Fig. 1 and Fig. 2, the angular velocity of each roller relative to the input disk is $\omega_{B0} = \omega_B - \omega_0$, while $\omega_{B1} = \omega_B - \omega_1$ is the one relative to the sun shaft, and $\omega_{B2} = \omega_B - \omega_2$ is the angular velocity of each roller relative to the output disk. The spin speed is defined as the normal component of the relative speed acting on the point of contact. After some geometrical considerations, we can define the spin coefficients as follows:

$$\sigma_{B0} = \tilde{r}_0 tan(\theta_0 + \gamma)(1 - C_{R0}) - sin(\theta_0) \tag{15}$$

$$\sigma_{B1} = \frac{k tan(\gamma)}{(1 - C_{R1})} \tag{16}$$

$$\sigma_{B2} = \frac{\tilde{r}_2 tan(\theta_2 - \gamma)}{(1 - C_{R2})} - sin(\theta_2) \tag{17}$$

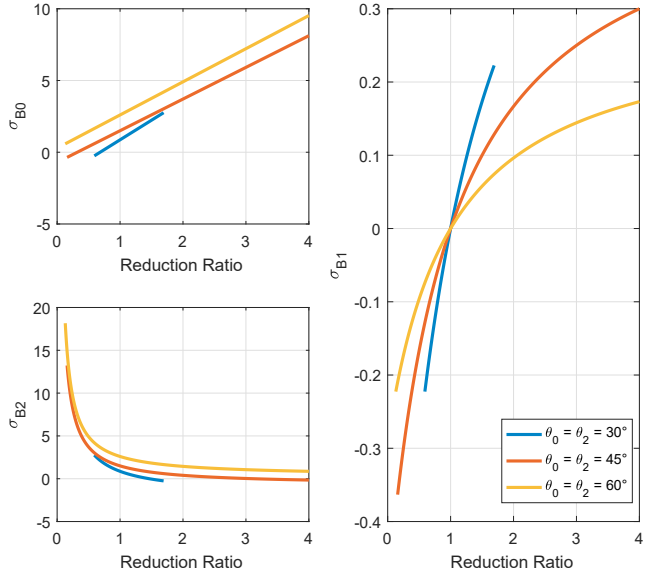

Fig. 4. Spin coefficients at different values of $\theta_0 = \theta_2$

Fig. 4 shows the spin coefficients as a function of the tilt angle. To perform these evaluations, we consider an aspect ratio of 0.5 and the simplifying hypothesis $\theta = \theta_0 = \theta_2$. By analysing these results, we can observe that there is a relevant amount of spin for each reduction ratio. In fact, there is no γ able to nullify spin coefficients in each contact point. Moreover, considering both Fig. 3 and Fig. 4, we can notice that the larger is the range of reduction ratio, the bigger is the amount of spin.

3. FORCES AND EFFICIENCY FORMULATION

The free body diagram in Fig. 5 allows us to perform an analysis of the force and torque equilibrium of the system. It is worth noting that the number of rollers is n. Moreover, we assume that the motor is linked to the disk 0, the load acts on the disk 2 and the sun is free to rotate. Tangential forces F_{B0}, F_{B1} and F_{B2} provide torque transmission through the rotating bodies. F_{D0} and F_{D2} are the clamping forces acting on the lateral disks. The normal forces F_{N0}, F_{N1} and F_{N2} provide high pressure contact between rollers and disks. The torque analysis must include the input and load torques, respectively T_0 and T_2. As stated before, the spin effect causes torque losses. T_{sp0}, T_{sp1} and T_{sp2} are the torques caused by spin phenomena. The bearing losses T_{BL0} and T_{BL1} act as load on the rollers and on the sun shaft. These friction torques are evaluated with reference to models from literature (Maldotti (2009), De Novellis et al. (2012)). These models represent the friction torque as the sum of two contributions: the load independent friction T_{B0}, and the load dependent friction T_{B1}. In particular, T_{B0} is a function of the bearing type, the lubrication method, and the rotational speed.

$$\begin{aligned} T_{B0} &= 160 \cdot 10^{-10} f_0 d^3 \quad \eta_c N < 2000 \\ T_{B0} &= 10^{-10} (\eta_c N)^{0.69} f_0 d^3 \quad \eta_c N > 2000 \end{aligned} \tag{18}$$

where $\eta_c [mm^2/s]$ is the kinematic viscosity of the lubricant, $N[rpm]$ is the rotational speed of the bearing, $d[mm]$ is the bearing mean diameter, and $f_0 = 12$ is a coefficient that depends on the bearing type.
The load dependent friction torque has been evaluated as follow:

$$T_{B1} = 10^{-3} f_1 P^a d_m^b \tag{19}$$

where $a = b = 1$, $f_1 = 3 \cdot 10^{-1}$ is a coefficient that depends on the bearing type and P is the equivalent load.
Force and torque equilibria on each roller give:

$$\begin{cases} F_{N1} = F_{N0} cos(\theta_0) + F_{N2} cos(\theta_2) \\ F_{N0} sin(\theta_0) + F_{N2} sin(\theta_2) = 0 \\ F_R + F_{B0} + F_{B1} - F_{B2} = 0 \end{cases} \tag{20}$$

$$\begin{aligned} T_{BL0} = F_{B0} r_{B0} - F_{B1} r_{B1} - F_{B2} r_{B2} + \\ + T_{sp0} sin(\theta_0 + \gamma) - T_{sp1} sin(\gamma) + T_{sp2} sin(\theta_2 - \gamma) \end{aligned} \tag{21}$$

$$\begin{aligned} T_R + F_{B0} r_B sin(\theta_0 + \gamma) - F_{B1} r_B sin(\gamma) + \\ - F_{B2} r_B sin(\theta_2 - \gamma) - T_{sp0} cos(\theta_0 + \gamma) + \\ + T_{sp1} cos(\gamma) + T_{sp2} cos(\theta_2 - \gamma) = 0 \end{aligned} \tag{22}$$

Considering the equilibrium of the input disk, the following relations hold true:

$$F_{Din} - n F_{N0} sin(\theta_0) = 0 \tag{23}$$

$$T_0 - n F_{B0} r_0 - n T_{sp0} sin(\theta_0) = 0 \tag{24}$$

The same analysis on output disk gives the following equations:

$$F_{Dout} - n F_{N2} sin(\theta_2) = 0 \tag{25}$$

$$T_2 + n F_{B2} r_2 - n T_{sp2} sin(\theta_2) = 0 \tag{26}$$

Considering that the sun shaft is free to rotate, the following relations hold true:

$$\sum_{i=1}^{n} F_{N1i} = 0 \tag{27}$$

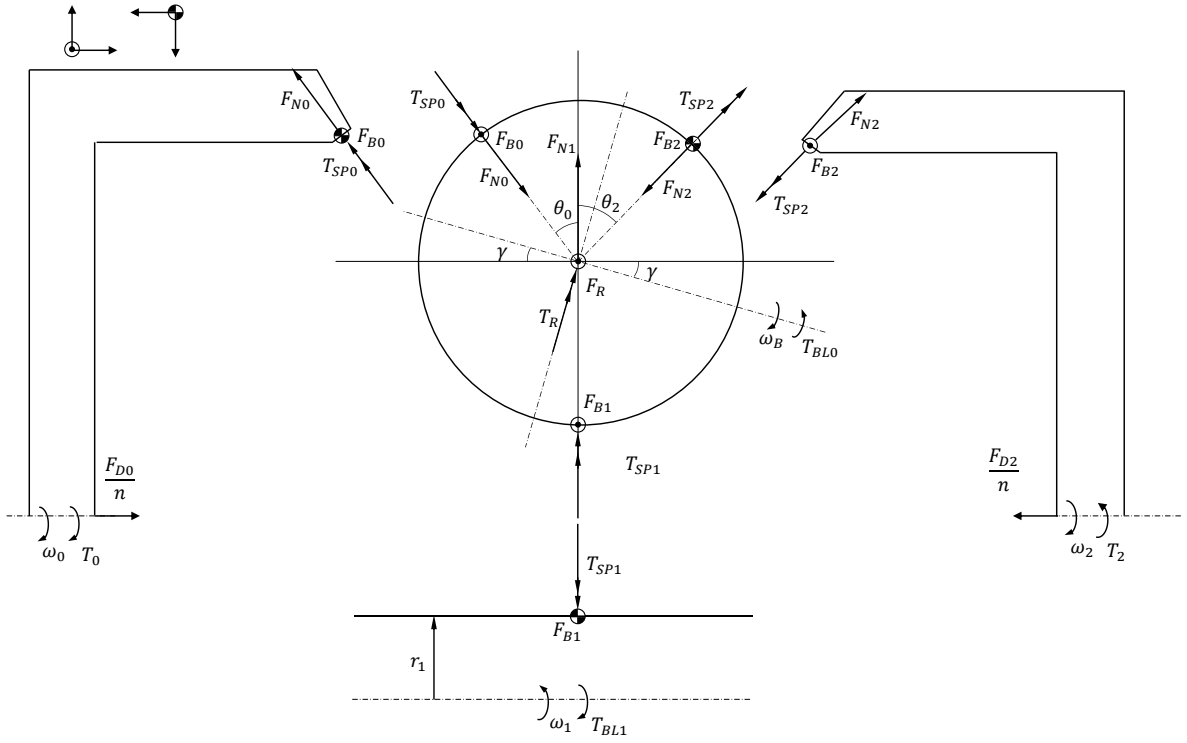

Fig. 5. Free body diagram of the transmission

$$T_{BL1} - nF_{B1}r_1 = 0 \tag{28}$$

Obviously, the sun shaft may be used as a second output shaft. In this case, the external torque acting on the sun shaft should be included in (28). Further considerations may be done only considering specific application becouse of the complexity of a double output trasmission.

3.1 Effiency

Considering the viscoelastic coupling between the elements, we can define the following traction coefficients:

$$\begin{aligned} \mu_0 &= F_{B0}/F_{N0} \\ \mu_1 &= F_{B1}/F_{N1} \\ \mu_2 &= F_{B2}/F_{N2} \end{aligned} \tag{29}$$

Similarly, we can define spin coefficients as follows:

$$\begin{aligned} \chi_0 &= T_{sp0}/(F_{N0}r_0) \\ \chi_1 &= T_{sp1}/(F_{N1}r_1) \\ \chi_2 &= T_{sp2}/(F_{N2}r_2) \end{aligned} \tag{30}$$

Using these coefficients in the simplifying condition $\theta = \theta_0 = \theta_2$, we can rephrase the torques balance as dimensionless quantities. Considering the disks equilibrium, the following relations hold true:

$$\begin{aligned} t_0 &= T_0/nr_0F_{N0} = \mu_0 + \chi_0 sin(\theta) \\ t_1 &= T_{BL1}/(nr_1F_{N1}) = \mu_1 \\ t_2 &= T_2/nr_2F_{N2} = -\mu_2 + \chi_2 sin(\theta) \end{aligned} \tag{31}$$

The equilibrium equation of the rollers in dimensionless form becomes:

$$\begin{aligned} t_B = T_B/F_{N0}r_b = \\ \tilde{r}_{B0}\mu_0 - 2cos(\theta)\tilde{r}_{B1}\mu_1 - \tilde{r}_{B2}\mu_2 + sin(\theta+\gamma)\tilde{r}_0\chi_0 - \\ 2cos(\theta)sin(\gamma)\tilde{r}_1\chi_1 + sin(\theta-\gamma)\tilde{r}_2\chi_2 \end{aligned} \tag{32}$$

Considering (8) and (14), we can define the efficiency in terms of speed and torque components:

$$\begin{aligned} \eta = \frac{P_2}{P_0} = \frac{T_2\omega_2}{T_0\omega_0} = \frac{T_2\omega_2\tau_{ID}}{T_0\omega_0\tau_{ID}} = \\ = \eta_{Speed}\frac{T_2 r_{B2} r_0}{T_0 r_{B0} r_2} = \eta_{Speed}\eta_{Torque} \end{aligned} \tag{33}$$

By Considering (8) and (31), the torque efficiency can be expressed as a function of the tilt angle:

$$\begin{aligned} \eta_{Torque} = \frac{T_{2R}}{T_{ID}} = -\tau_{ID}\frac{t_2 nF_{N2}r_2}{T_0} = \\ = -\tau_{ID}\frac{t_2 nF_{N2}r_2}{t_0 nF_{N0}r_0} = \tau_{ID}\frac{[\mu_2 - \chi_0 sin(\theta)]}{[\mu_0 + \chi_0 sin(\theta)]} \end{aligned} \tag{34}$$

Finally, global efficiency is:

$$\begin{aligned} \eta = \eta_{Speed}\eta_{Torque} = \\ = \frac{[\mu_2 - \chi_0 sin(\theta)]}{[\mu_0 + \chi_0 sin(\theta)]}\tau_{ID}(1 - C_{R0})(1 - C_{R2}) \end{aligned} \tag{35}$$

4. CONTACT MODEL

The contact model considered in this work has been developed using the model proposed in Carbone et al. (2007), De Novellis et al. (2012). The authors proposed a procedure that enables the evaluation of the coefficients in (29) and (30) in fully flooded isothermal hard-EHL contacts. Due to the high pressure distribution (1-3 GPa), and by assuming fluid film thickness is constant in the contact region, we can apply the results from Hertzian theory Hamrock (1994). The pressure distribution is evaluated considering the curvature radii and the axes length of the elliptic conjunction in the point of contact. Finally, the shear stress in the fluid film has been computed considering the viscosity and the film thickness of the traction oil. These quantities are evaluated considering the difference between the tangential velocities of the contacting bodies in the region of contact using equations (10), (11) and (12). By using the definition in (29) and (30) for an infinitesimal section of the contact region, and then integrating along the elliptic contact using polar coordinates, it follows:

$$\mu_0 = \tilde{a}_{X0}\tilde{a}_{Y0}\int_0^1 dR\int_0^{2\pi}\tilde{\tau}_{B0x}Rd\psi \tag{36}$$

$$\mu_1 = -\tilde{a}_{X1}\tilde{a}_{Y1}\int_0^1 dR\int_0^{2\pi}\tilde{\tau}_{B1x}Rd\psi \tag{37}$$

$$\mu_2 = -\tilde{a}_{X2}\tilde{a}_{Y2}\int_0^1 dR\int_0^{2\pi}\tilde{\tau}_{B2x}Rd\psi \tag{38}$$

$$\chi_0 = \frac{\tilde{a}_{X0}\tilde{a}_{Y0}}{\Re_0\tilde{r}_0}\int_0^1 dR\int_0^{2\pi}\phi_0(\psi)R^2d\psi \tag{39}$$

$$\chi_1 = \frac{\tilde{a}_{X1}\tilde{a}_{Y1}}{\Re_1\tilde{r}_1}\int_0^1 dR\int_0^{2\pi}\phi_1(\psi)R^2d\psi \tag{40}$$

$$\chi_2 = \frac{\tilde{a}_{X2}\tilde{a}_{Y2}}{\Re_2\tilde{r}_2}\int_0^1 dR\int_0^{2\pi}\phi_2(\psi)R^2d\psi \tag{41}$$

where $\phi_i(\psi) = (\tilde{\tau}_{Biy}cos(\psi) - \tilde{\tau}_{Bix}sin(\psi))$, $\tilde{\tau}_{Bix}$ and $\tilde{\tau}_{Biy}$ are respectively, the shear stress along the rolling direction and along the normal direction for each point of contact. $\Re$ is the load factor that depends on the geometry and the normal force. $\tilde{a}_X$ and $\tilde{a}_Y$ are the axes length of the elliptic contact in dimensionless form.

5. SIMULATION RESULTS

The aim of the proposed model is to evaluate the efficiency of a planetary CVT. To perform a simulation of the model, it is necessary to define a set of geometrical parameters, the fluid properties and the operative point of the transmission. Table 1 contains the geometrical quantities of the considered transmission. To analyse the creep and spin effects, the efficiency results are provided in terms of speed and torque efficiency as function of the input torque at different reduction ratios. The fluid properties considered in this model are the same as in De Novellis et al. (2012). In simulations, the input speed has been chosen equal to $\omega_0 = 2000rpm$, while the power request ranges in $[0.01 - 12]kW$. Finally, clamping forces are chosen in order to obtain $F_{N0} = 1.5kN$.

Aspect ratio	$k = 0.5$
Roller radius	$r_b = 0.05m$
Half cone angle disk0-roller	$\theta_0 = 45$
Half cone angle disk2-roller	$\theta_2 = 45$

Table 1. Geometrical parameters

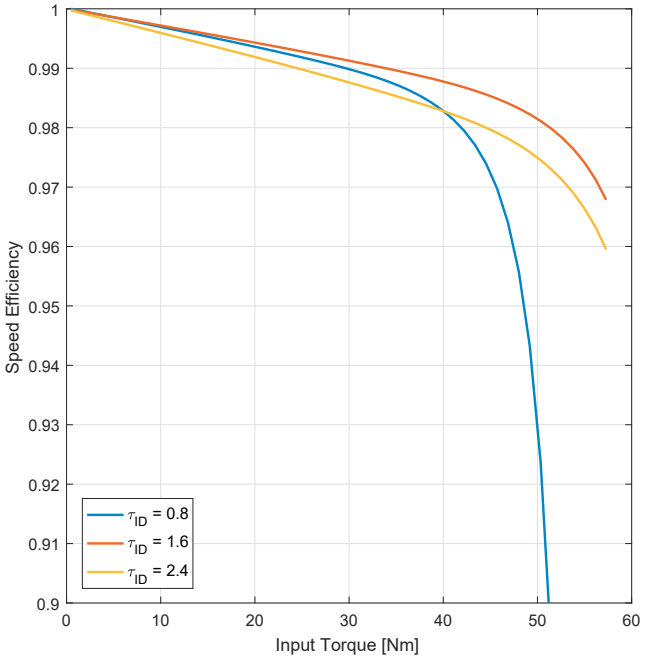

Fig. 6. Speed efficiency as a function of input torque at different transmission ratio

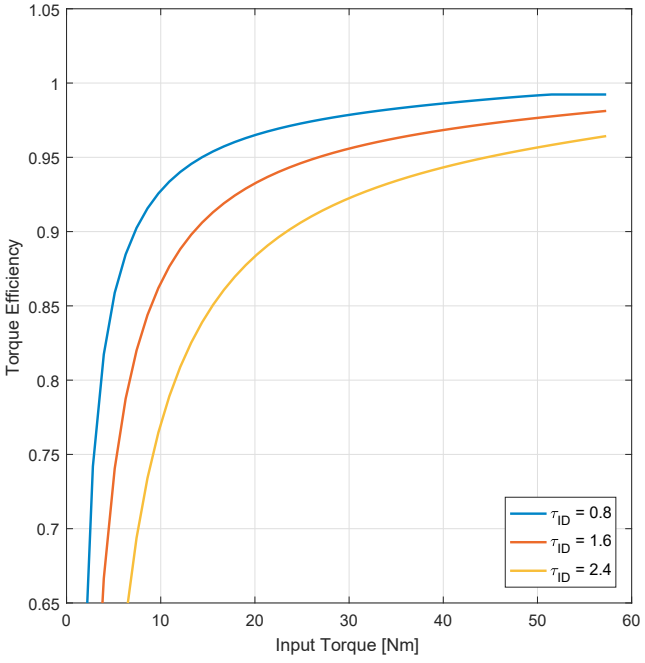

Fig. 7. Torque efficiency as a function of input torque at different transmission ratio

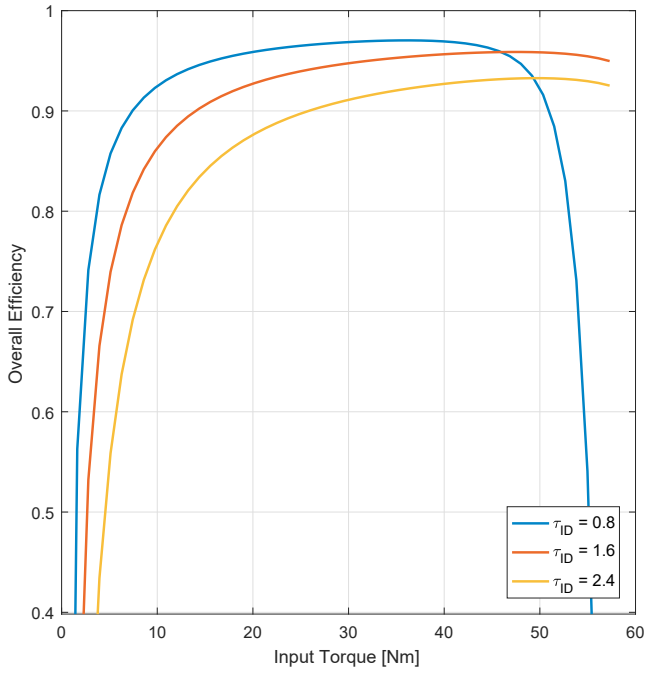

Fig. 8. Efficiency as a function of input torque at different transmission ratio

The curves in Fig. (6) show that the speed efficiency decreases at high torque. This is due to the high creep needed to generate the tangential forces in the rolling direction. Obviously, high slip produces a high loss in terms of speed efficiency. Morover, clamping forces can be adjusted to improve speed efficiency at high torque demand, but this means additional devices and additional costs to be evaluated in the design phase. In Fig. (7) we can observe the losses in terms of torque. Comparing these curves with Fig. (4), we can observe that the higher is the transmission ratio, the higher are the spin coefficients. Due to the duality between creep losses and spin losses, the overall efficiency has the behaviour shown in Fig. (8). In the middle part of the operative region, the efficiency is higher than 90%.

6. CONCLUSION

In this paper, we presented a mathematical model of a novel type of CVT. The proposed model considers the EHL contact enabling the transfer of the torque through the transmission. The model allows the computation of the efficiency curves for different geometrical parameters at different operative points. Moreover, the model can be used during the design process to optimize the geometry of the CVT for a given application. In fact, an efficient and optimized design of this kind of transmission in powertrain applications requires a proper representation of phenomena like spin and creep. The comparison of the proposed transmission with the toroidal trasmission shows similar efficiency performances. Nevertless, from the free body diagram, we can observe that clamping forces have no effect on the reduction ratio shift mechanism. This means that the shift ratio mechanism could be simpler and faster then the one of the toroidal variator. Finally, the proposed model is the starting point for developing a dynamic model of the transmission.

REFERENCES

Bottiglione, F., De Pinto, S., Mantriota, G., and Sorniotti, A. (2014). Energy consumption of a battery electric vehicle with infinitely variable transmission. *Energies*, 7, 8317–8337.

Carbone, G., Mangialardi, L., Bonsen, B., Tursi, C., and Veenhuizen, P. (2007). CVT dynamics: Theory and experiments. *Mechanism and Machine Theory*, 42(4), 409 – 428.

Carbone, G., Mangialardi, L., and Mantriota, G. (2001). Fuel consumption of a mid class vehicle with infinitely variable transmission. *SAE International Journal of Engines*, 110, 2474–2483.

De Novellis, L., Carbone, G., and Mangialardi, L. (2012). Traction and efficiency performance of the double roller full-toroidal variator: A comparison with half- and full-toroidal drives. *Journal of Mechanical Design, Transactions Of the ASME*, 134(7).

Hamrock, B.J. (1994). *Fundamentals of Fluid Film Lubrication (The McGraw-Hill series in mechanical engineering)*. McGraw-Hill.

Loewenthal, S.H. (1986). Spin analysis of concentrated traction contacts. *Journal of mechanisms, transmissions, and automation in design*, 108(1), 77–85.

Maldotti, S. (2009). *Sulla energia dissipata in alcuni organi di macchina*. Ph.D. thesis, Alma Mater Studiorum.

S. Cretu, O. and P. Glovnea, R. (2003). Traction drive with reduced spin losses. *Journal of Tribology-transactions of The Asme - J TRIBOL-TRANS ASME*, 125. doi: 10.1115/1.1538192.

Verbelen, F., Derammelaere, S., Sergeant, P., and Stockman, K. (2018). A comparison of the full and half toroidal continuously variable transmissions in terms of dynamics of ratio variation and efficiency. *Mechanism and Machine Theory*, 121, 299 – 316.